Lack of Arginine Vasopressin–Induced Phosphorylation of Aquaporin-2 Mutant AQP2-R254L Explains Dominant Nephrogenic Diabetes Insipidus

Fabrizio de Mattia,* Paul J.M. Savelkoul,* Erik-Jan Kamsteeg,* Irene B.M. Konings,* Peter van der Sluijs,† Rudolf Mallmann,‡ Alexander Oksche,§‖ and Peter M.T. Deen*

**Department of Physiology, Radboud University Nijmegen Medical Center, Nijmegen, The Netherlands; †Department of Cell Biology, UMC Utrecht, Utrecht, The Netherlands; ‡Elisabeth-Krankenhaus, Essen, Germany; §Institut für Pharmakologie, Charité, Campus Benjamin Franklin, Berlin, Germany; and ‖Forschungsinstitut fur Molekulare Pharmakologie, Campus Berlin Buch, Berlin, Germany*

Water homeostasis in humans is regulated by vasopressin, which induces the translocation of homotetrameric aquaporin-2 (AQP2) water channels from intracellular vesicles to the apical membrane of renal principal cells. For this process, phosphorylation of AQP2 at S256 by cAMP-dependent protein kinase A is thought to be essential. Mutations in the AQP2 gene cause recessive and dominant nephrogenic diabetes insipidus (NDI), a disease in which the kidney is unable to concentrate urine in response to vasopressin. Here, a family in which dominant NDI was caused by an exchange of arginine 254 by leucine in the intracellular C terminus of AQP2 (AQP2-R254L), which destroys the protein kinase A consensus site, was identified. Expressed in oocytes, AQP2-R254L appeared to be a functional water channel but was impaired in its transport to the cell surface to the same degree as AQP2-S256A, which mimics nonphosphorylated AQP2. In polarized renal cells, AQP2-R254L was retained intracellularly and was distributed similarly as AQP2-S256A or wild-type AQP2 in unstimulated cells. Upon co-expression in MDCK cells, AQP2-R254L interacted with and retained wild-type AQP2 in intracellular vesicles. Furthermore, AQP2-R254L had a low basal phosphorylation level, which was not increased with forskolin, and mimicking constitutive phosphorylation in AQP2-R254L with the S256D mutation shifted its expression to the basolateral and apical membrane. These data indicate that dominant NDI in this family is due to a R254L mutation, resulting in the loss of arginine vasopressin–mediated phosphorylation of AQP2 at S256, and illustrates the *in vivo* importance of phosphorylation of AQP2 at S256 for the first time.

J Am Soc Nephrol 16: 2872–2880, 2005. doi: 10.1681/ASN.2005010104

In hypernatremia or hypovolemia, arginine vasopressin (AVP) release from the pituitary is increased to restore a proper water balance. In renal collecting ducts, AVP will bind to the vasopressin-2 receptor (AVPR2) located in the basolateral membrane, which will induce a transient increase in intracellular cAMP, which in turn increases protein kinase A (PKA) activity. PKA then is thought to phosphorylate several proteins, including aquaporin-2 (AQP2) water channels, which reside in intracellular vesicles. Phosphorylated AQP2 (p-AQP2) then redistributes to the apical membrane, which renders the cells water permeable. Driven by the transcellular osmotic gradient, water from the glomerular filtrate then enters the cells *via* AQP2 and leaves the cells to the interstitium *via* AQP3 and AQP4, located in the basolateral membrane, thereby restoring isotonicity and euvolemia (1,2).

Mutations in the *AQP2* gene cause autosomal recessive and dominant nephrogenic diabetes insipidus (NDI), a disease in which the kidney is resistant to the action of AVP (3,4). Expression studies revealed that AQP2 mutants in dominant NDI are properly folded but are missorted. This sorting defect is also present in heteroligomers of mutant and wild-type (wt) AQP2, which explains the dominant negative effect. Depending on the mutation, however, the mutants in dominant NDI are missorted to different subcellular destinations (5–10). Data on the molecular mechanisms underlying dominant NDI might provide novel cell biologic information on protein sorting and will broaden our insight on critical elements in the AQP2 protein.

In this study, we identified a novel mutation in one allele of a family with dominant NDI, which encodes an AQP2-R254L mutant protein. For identifying whether AQP2-R254L can be causal to NDI and for determining the underlying mechanism of this mutation in dominant NDI in this family, AQP2-R254L was expressed in oocytes and polarized epithelial MDCK cells and analyzed in detail.

Received January 25, 2005. Accepted July 8, 2005.

Published online ahead of print. Publication date available at www.jasn.org.

F.d.M. and P.J.M.S. contributed equally to this work.

Address correspondence to: Dr. Peter M.T. Deen, Department of Cell Physiology, Radboud University Nijmegen Medical Center, 160, P.O. Box 9101, 6500 HB Nijmegen, The Netherlands. Phone: 31-243617347; Fax: 31-243616413; E-mail: p.deen@ncmls.ru.nl

ISSN: 1046-6673/1610-2872

Materials and Methods

Analysis of the Patient with NDI

Clinical analyses of inulin and para-amino hippuric acid clearance; blood and urine osmolalities; and levels of sodium, potassium, urea, and creatinine were done by standard procedures. The V2R and *AQP2* gene of the patient and her mother were sequenced as described (11,12).

Constructs

The constructs encoding pT7Ts-AQP2, pT7Ts-AQP2-R187C, pT7Ts-AQP2-S256A, pT7Ts-wt-AQP2-F, and G-AQP2 were as described (3,5,7,13). The cDNA coding for pT7Ts-AQP2-R254L was made by introducing the mutations into pT7Ts-AQP2 with the Altered Sites mutagenesis kit (Promega, Madison, WI) using the primer 5′-CGAG-GTGCGACGTC*TG*CAGTCGGTGG-3′. Introduction of only the desired mutations was confirmed by DNA sequence analysis. For generating pCB6-AQP2-R254L, the AQP2-R254L coding sequence was digested from pT7Ts-AQP2-R254L with *Bgl*II and SpeI and ligated into the *Bgl*II and XbaI sites of the eukaryotic expression vector pCB6.

For generating a FLAG (DYKDDDDK)-tagged AQP2-R254L expression construct, pBluescript-FLAG-AQP2 (7) was cut with NotI, blunted and digested with HindIII, and the FLAG-tagged AQP2 (F-AQP2) cDNA fragment was isolated. In pCB7, which is similar to pCB6 but contains a hygromycin instead of neomycin resistance gene, the BamHI site was cut, blunted, and re-ligated. Next, the F-AQP2 fragment was ligated into the blunted KpnI site and the HindIII of pCB7-ΔBamHI to yield pCB7-ΔBamHI-F-AQP2. For generating pCB7-F-AQP2-R254L, pT7Ts-AQP2-R254L was digested with BamHI and KpnI, a 300-bp fragment isolated and cloned into the corresponding sites of pCB7-ΔBamHI-F-AQP2.

Oocytes

The pT7Ts-AQP2 constructs were linearized with SalI. Subsequent transcription and analysis of the integrity of the obtained cRNA was done as described (5). cRNA injection of oocytes and analysis of their water permeabilities were done as reported (3). Statistical significance was determined using the *t* test and was considered significant at $P < 0.05$. Total and plasma membranes were isolated 2 d after cRNA injection as described (14).

MDCK Cells

MDCK cells were cultured and stably transfected with the expression constructs as described (15). Selection of G418-resistant clones and immunocytochemistry of transfected MDCK cells were done as described (16). MDCK cell lines that stably expressed wt-AQP2 (wt-10), AQP2-S256A, or green fluorescent protein (GFP)–tagged AQP2 were as described (13,17,18).

MAb against FLAG (m2) and early endosomal antigen-1 (EEA1) were purchased from Sigma (St. Louis, MO), and BD Transduction Laboratories (Lexington, KY), respectively. Polyclonal antibodies against the Golgi marker proteins GOS28 and Giantin and the endoplasmic reticulum (ER) marker protein disulphide isomerase were provided by Dr. Y. Ikehara (Fukuoka University School of Medicine, Fukuoka, Japan) and Dr. Ineke Braakman (University of Utrecht, Utrecht, The Netherlands). MAb (clone AC17) against the late endosomal/lysosomal marker protein Lamp2 were provided by Dr. Le Bivic (Marseille, France). Anti-rabbit and anti-mouse secondary antibodies coupled to Alexa 488 or 594 were obtained from Molecular Probes (Eugene, OR). Images were obtained with a Bio-Rad (Hercules, CA) confocal laser-scanning microscope (CLSM) using a ×60 oil-immersion objective and a three-fold magnification. Orthophosphate labeling of MDCK cells, immunoprecipitation, and immunoblotting were performed as described (18). Transient transfections have been performed using LipofectAMINE 2000 reagent (Invitrogen Life Technologies, Paisley, UK) according to the manufacturer's protocol.

Immunoprecipitation of FLAG-AQP2-R254L Proteins

Binding of monoclonal anti-FLAG antibodies (M2; Sigma) to protein G–agarose beads (Amersham Pharmacia Biotech AB, Uppsala, Sweden) was done as described (7). MDCK cells were grown to confluence in six-wells plates, Well equivalents of cells were scraped in 2 ml of PBS with 0.02% EDTA, spun down for 5 min at 200 × *g* at 4°C, and homogenized in HbA (20 mM Tris [pH 7.4], 5 mM $MgCl_2$, 5 mM NaH_2PO_4, 1 mM EDTA, 80 mM sucrose, 1 mM PMSF, and 5 μg/ml leupeptin and pepstatin) using a pestle. Unbroken cells and nuclei were removed by centrifugation for 10 min at 10 × *g* at 4°C. Membranes were spun down for 1 h at 16,000 × *g* at 4°C. Membranes were solubilized either in Laemmli buffer (total membranes) or in 1 ml of solubilization buffer (4% deoxycholate, 20 mM Tris [pH 8.0], 5 mM EDTA, 10% glycerol, 1 mM PMSF, and 5 μg/μl leupeptin and pepstatin) and incubated for 1 h at 37°C. Then the solubilized membranes were rotated overnight with the protein G beads coupled to anti-FLAG antibodies. After three washes, the immunoprecipitated proteins were solubilized in Laemmli buffer and analyzed by immunoblotting.

Densitometric Analysis

For relating the phosphorylation level of AQP2-R254L with that of wt-AQP2, immunoblot and [^{32}P]orthophosphate signals were semi-quantified by measuring the integrated optical densities (IOD) of the film signals using the Image-Pro Plus analysis software (Media Cybernetics, Silver Springs, CO). These signals were compared with those of two-fold dilution series of wt-AQP2, which were blotted, or separated by SDS-PAGE and autoradiographed, in parallel. Background IOD values were determined at unexposed areas of the film and subtracted from obtained IOD values for the different proteins. For determining the relative levels of phosphorylation, the phosphorylation signals were normalized for the corresponding amounts of immunoprecipitated AQP2 and expressed as a percentile of phosphorylated wt-AQP2 protein detected under unstimulated conditions.

Results

Analyses of the Patient

The proband presented with polyuria and polydipsia within the first year of life. NDI was diagnosed at the age of 12. At that time, the patient weighed 48.5 kg, was 150 cm in height, and had a urinary volume between 4.2 and 7.9 L/24 h, which thus corresponded to 87 to 163 ml/kg body wt per d. The specific weight of the urine was in the range of 1003 and 1005 g/L. Inulin and para-amino hippuric acid clearance were normal. Upon infusion of 2.5% NaCl, the specific weight and urinary osmolality increased to 1012 g/L and 452 mOsmol/L, respectively.

The patient then was treated with hydrochlorothiazide, starting with 12.5 mg three times daily and later with 25 mg twice daily. Under this treatment, water intake was approximately 1.5 and 3 L/24 h, and the specific weight of the urine raised to 1018 g/L. The father of the index patient, who has passed away, also had a history of polydipsia and polyuria and low urinary osmolality of 182 mOsmol/L. Upon administration of vasopressin, his UOsm increased only slightly (241 mOsmol/L). The mother was not affected.

The male patient is now 51 yr of age and has mental retardation, most likely as a result of recurrent hypernatremic episodes, and has type 2 diabetes. He is treated with hydrochlorothiazide (25 mg twice daily) and supplemented with potassium. His current water intake amounts 5 to 6 L/24 h, which corresponds to 55 to 65 ml/kg body wt per day.

Because mutations in the X-linked *AVPR2* gene are the most common cause of congenital NDI, its coding sequence in the proband was determined. However, no mutation was found. Subsequent genomic analysis of the *AQP2* gene of the proband revealed a mutation in one allele (G761T), which leads to an AQP2 protein in which Arg254 is exchanged for a Leu (AQP2-R254L). This mutation was not observed in the AQP2 gene of >80 healthy individuals. The *AQP2* genes of the mother revealed no mutation (Figure 1).

Functional Analysis of AQP2-R254L in Oocytes

For determining whether the identified missense mutation could be the underlying cause for NDI in this family, the mutation was introduced into the AQP2 cDNA sequence, cloned into an oocyte expression vector, and transcribed. Because R254 in AQP2 is part of the PKA phosphorylation consensus site (R-R$_{254}$-X-S), we hypothesized that the R254L mutation in AQP2 might interfere with proper phosphorylation of S256 and plasma membrane expression of the protein, as AQP2-S256A, which mimics nonphosphorylated AQP2, is retained in vesicles in oocytes and in mammalian cells (18–21).

Subsequently, oocytes were injected with different amounts of cRNA encoding wt-AQP2 or with 0.3 ng of cRNA encoding either AQP2-R254L or AQP2-S256A. Determination of the water permeabilities (Pf) revealed that AQP2-R254L is a functional water channel, because the Pf of oocytes that expressed AQP2-R254L (22.8 ± 6.8; $n = 8$) was significantly higher than those of controls (8.9 ± 4.9; $n = 8$; $P < 0.005$; Figure 2A). To determine whether the reduced Pf of AQP2-R254L-expressing oocytes was due to an impaired transport of AQP2-R254L to the plasma membrane, we isolated total membranes and plasma membranes from the same batches of oocytes. Subsequent AQP2 immunoblotting revealed that the total expression of AQP2-R254L was in between that of oocytes that were injected with 0.1 and 0.3 ng of wt-AQP2 cRNA (Figure 2B, TM) but that its plasma membrane expression level was less than that of oocytes injected with 0.1 ng of wt-AQP2 cRNA (Figure 2B, PM). These data indicated that AQP2-R254L was impaired in its trafficking to the plasma membrane and thus that the R254L mutation was likely to cause NDI in this family. It is interesting that the total and plasma membrane expression as well as the Pf of AQP2-R254L and AQP2-S256A were similar, which indicated that the molecular cause for AQP2-R254L in dominant NDI indeed could be the lack of S256 phosphorylation. As shown for AQP2-S256A (5,20), functional AQP2 mutants in recessive NDI (13,22,23), a retained AQP2 mutant in dominant NDI (AQP2-E258K [7,22]), and also here for wt-AQP2 (Figure 2), the conferred water permeability for AQP2-R25L was related directly to its expression level (Figure 2C).

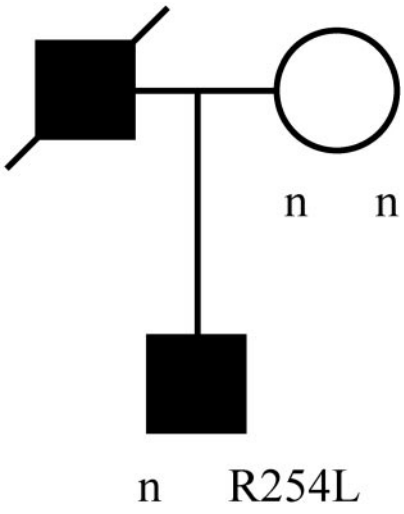

Figure 1. Inheritance of nephrogenic diabetes insipidus (NDI) in the studied family. Healthy (open symbols) and affected individuals (closed symbols), male (squares) or female (circles) individuals, and the aquaporin 2 (AQP2) mutation or normal (n) allele are indicated. A slashed symbol indicates a deceased individual.

AQP2-R254L Heteroligomerizes with wt-AQP2

AQP2 mutants in dominant but not recessive NDI are able to exit the ER and exert their dominant negative effect by forming heteroligomers with wt-AQP2 (6–8,10). For determining whether AQP2-R254L forms heteroligomers with wt-AQP2, membranes of oocytes that expressed FLAG-tagged wt-AQP2 (F-AQP2) alone or in combination with wt-AQP2, AQP2-R254L, or AQP2-R187C (a mutant in recessive NDI) were solubilized and subjected to immunoprecipitation using FLAG antibodies. Immunoblotting of total membranes for AQP2 revealed a 31-kD band representing F-AQP2; a 29-kD band corresponding to untagged wt-AQP2, AQP2-R254L, and AQP2-R187C; and a 32-kD band corresponding to high-mannose glycosylated AQP2-R187C (Figure 2D, TM). Immunoblot analysis of the immunoprecipitates revealed that wt-AQP2 and AQP2-R254L co-precipitated with F-AQP2 (Figure 2D, IP). As reported (7), AQP2-R187C did not oligomerize with wt-AQP2. No AQP2 was detected in the immunoprecipitates from oocytes that expressed AQP2 only, which showed the specificity of the immunoprecipitations for FLAG-tagged proteins. From these results, it was concluded that AQP2-R254L forms heteroligomers with wt-AQP2.

Localization and Translocation of AQP2-R254L in MDCK Cells

As oocytes are not polarized (as collecting duct cells) and we were not able to study AQP2 phosphorylation in these cells, polarized MDCK cells were transfected with a eukaryotic expression construct encoding AQP2-R254L. MDCK cells do not endogenously express AQP2, but MDCK cells that stably express human AQP2 (MDCK-AQP2 cells) show a proper regulation of AQP2 translocation by forskolin and AVP (17). Single MDCK-AQP2-R254L clones were grown to confluence, incubated with or without forskolin, and subjected to AQP2 immu-

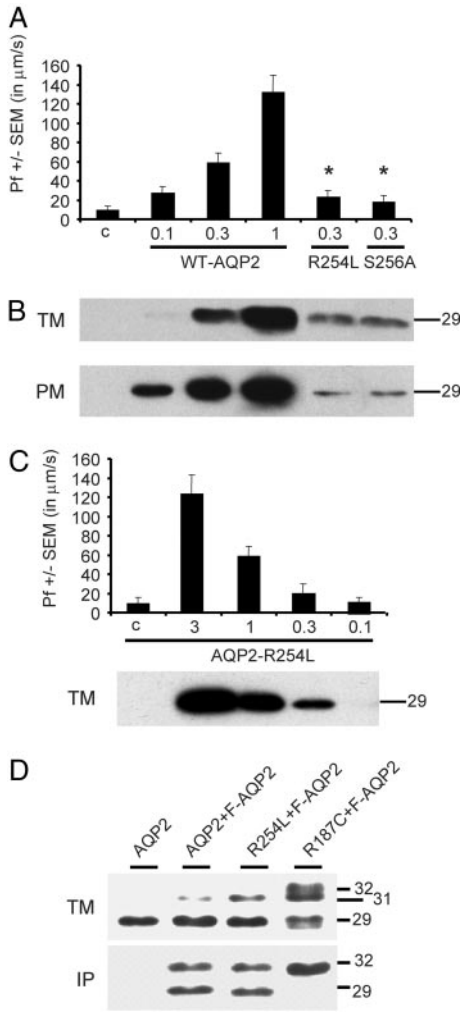

Figure 2. Functional analysis and expression of AQP2-R254L in oocytes. The *x* axis of A also applies for B. (A) Water permeability in oocytes. Three days after injection of the indicated amounts of wild-type (wt)-AQP2, AQP2-R254L, or AQP2-S256A cRNA (in ng), oocytes were subjected to a standard swelling assay. Noninjected oocytes were taken as a control (c). Mean water permeabilities (Pf) and SEM of eight oocytes are shown. Significant differences in water permeability compared with control oocytes are indicated by asterisks. (B) AQP2 expression in oocytes. From 12 oocytes injected as described above, total membranes (TM) or plasma membranes (PM) were isolated. Subsequently, equivalents of one (TM) or four (PM) oocytes were immunoblotted for AQP2. Molecular masses (in kD) are indicated on the right. (C) Relation between AQP2-R254L expression and water permeability. Of oocytes that were injected with different amounts of AQP2-R254L cRNA (indicated; in ng) or noninjected oocytes (c), the water permeability (Pf) was measured, and the expression in TM was determined as described above. (D) Heteroligomerization of AQP2-R254L with wt-AQP2. Of 30 oocytes, expressing AQP2 alone or a combination of F-AQP2 with wt-AQP2, AQP2-R254L, or AQP2-R187C, TM were isolated. Equivalent fractions were solubilized in deoxycholate and subjected to immunoprecipitation (IP) using anti-FLAG antibodies. Subsequently, TM and IP were immunoblotted for AQP2. The molecular masses of high-mannose glycosylated AQP2 (32), unglycosylated (29) AQP2, and FLAG-tagged AQP2 (31) are indicated in kD on the right.

nocytochemistry. CLSM revealed that AQP2-R254L localized to intracellular vesicles, which was not changed upon incubation with forskolin (Figure 3, top). In contrast, forskolin treatment of MDCK-AQP2 cells resulted in the translocation of wt-AQP2 from intracellular vesicles to the apical membrane (Figure 3, bottom). It is interesting that in unstimulated MDCK-AQP2 and MDCK-AQP2-R254L cells, the distribution of AQP2 seemed similar to that found for AQP2-S256A (18). Therefore, for identifying the subcellular organelles in which AQP2-R254L resides, MDCK cells that expressed wt-AQP2, AQP2-R254L, or AQP2-S256A were tested for co-localization with marker proteins for the ER (protein disulphide isomerase), cis-Golgi (GOS28), medial-trans-Golgi (Giantin), early endosomes (EEA1), or late endosomes/lysosomes (Lamp2). However, none of the studied AQP2 proteins seemed to co-localize with the marker proteins (data not shown), except for EEA1, which partially co-localized with all three proteins (Figure 4A, arrows).

AQP2-R254L Impairs Trafficking of wt-AQP2 to Apical Membrane

Because AQP2-R254L was retained in intracellular vesicles in MDCK cells, we next wanted to investigate whether AQP2-R254L exhibits a dominant negative effect on the trafficking of GFP-tagged AQP2 (G-AQP2). For obtaining cells that express G-AQP2 alone as well as together with FLAG-tagged AQP2-R254L (F-AQP2-R254L), F-AQP2-R254L was transiently expressed in MDCK cells that stably expressed G-AQP2. Immunocytochemistry and CLSM analysis of monolayers revealed that in cells that co-expressed G-AQP2 and AQP2-R254L, the

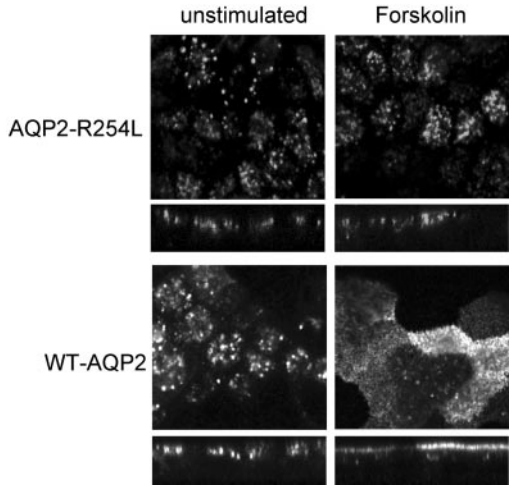

Figure 3. Localization of wt-AQP2 and AQP2-R254L in MDCK cells. MDCK cell lines that stably expressed AQP2-R254L or wt-AQP2 (indicated) were grown to confluence on semipermeable filters and incubated overnight with indomethacin to reduce basal cAMP levels (unstimulated; left). Subsequently, cells were stimulated for 45 min with forskolin in the presence of indomethacin (forskolin; right). After fixation and permeabilization, the cells were incubated with rabbit anti-AQP2 antibodies, followed by Alexa 488–conjugated anti-rabbit antibodies, and analyzed by confocal laser scanning microscopy (CLSM).

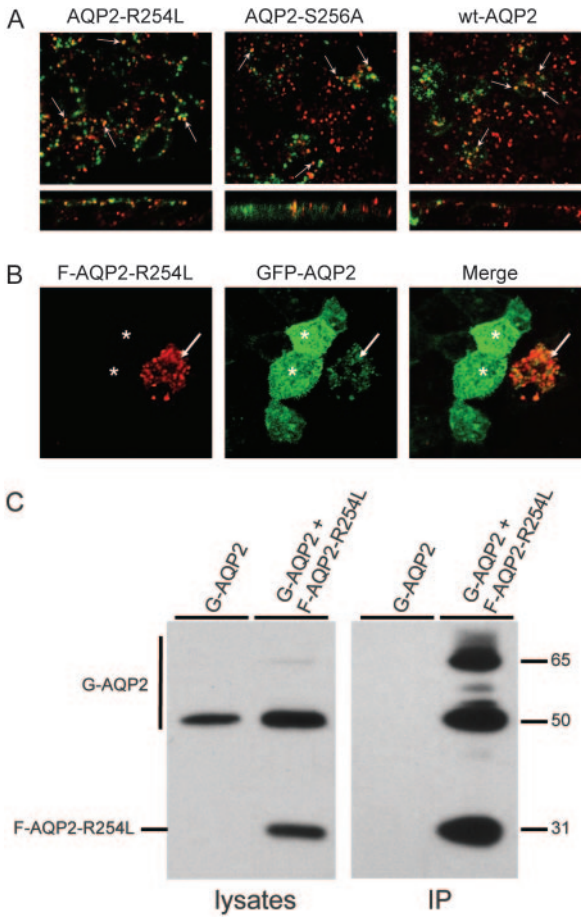

Figure 4. (A) Localization of AQP2-R254L to early endosomes. MDCK cells stably expressing wt-AQP2, AQP2-R254L, or AQP2-S256A were grown and treated as unstimulated cells described in the legend of Figure 3. Next, the cells were fixed, permeabilized, and immunostained for AQP2 and early endosomal antigen-1 (EEA1) and subjected to CLSM analysis. Co-localization of EEA1 (red) and AQP2 (green) are indicated by arrows. (B) AQP2-R254L impairs sorting of wt-AQP2 to the apical membrane. MDCK cells that stably expressed green fluorescent protein (GFP)–tagged wt-AQP2 (GFP-AQP2) were transiently transfected with a FLAG-tagged AQP2-R254L (F-AQP2-R254L) expression construct and grown and treated as described in the legend of Figure 3. After fixation and permeabilization, cells were immunostained with FLAG antibodies and analyzed by CLSM. Upon co-expression, G-AQP2 (green) and F-AQP2-R254L (red) co-localize in intracellular vesicles (arrows), whereas G-AQP2 alone is expressed in the apical membrane (*). (C) F-AQP2-R254L heteroligomerizes with G-AQP2 in MDCK cells. Solubilized membranes from cells expressing G-AQP2 alone or F-AQP2-R254L and G-AQP2 were isolated and split into two equivalent fractions. After solubilization and immunoprecipitation with FLAG antibodies, both the lysates and IP samples were immunoblotted for AQP2. The masses of G-AQP2 and F-AQP2-R254L are indicated in kDa on the right.

proteins co-localized in intracellular vesicles (Figure 4B; arrow). In contrast and as reported before (13), cells that expressed only G-AQP2 showed a dispersed expression pattern, which is typical for apical membrane expression (Figure 4B, asterisks). For revealing the heteromeric AQP2 interaction biochemically, cells that stably expressed either G-AQP2 or G-AQP2 and F-AQP2-R254L were subjected to immunoprecipitations using anti-FLAG antibodies. Immunoblot analysis of the immunoprecipitates with GFP antibodies showed that G-AQP2 co-precipitated with F-AQP2-R254L (Figure 4C, IP), whereas the cells that expressed G-AQP2 only do not show any signal. These data revealed that AQP2-R254L interacts with and impairs the trafficking of wt-AQP2 to the apical membrane.

Phosphorylation of AQP2-R254L in MDCK Cells

For testing whether the retention of AQP2-R254L in MDCK cells is due to a lack of S256 phosphorylation, MDCK cells that expressed wt-AQP2, AQP2-R254L, or AQP2-S256A were subjected to orthophosphate labeling in the presence or absence of forskolin. Indomethacin was used in all samples to reduce intracellular cAMP levels and basal AQP2 phosphorylation (17). Subsequently, AQP2 proteins were immunoprecipitated, and equivalents were loaded on a gel and exposed to a film for 3 d (Figure 5A, ^{32}P) or immunoblotted for AQP2 (Figure 5A, IB). Analysis of the autoradiogram revealed that wt-AQP2 and AQP2-R254L are already phosphorylated in the absence of forskolin stimulation. In contrast, AQP2-S256A was not phosphorylated, even though these cells were stimulated with forskolin and AQP2-S256A was expressed at high levels.

Upon stimulation with forskolin, no increase in the level of phosphorylation was observed for AQP2-R254L, in contrast to wt-AQP2. Densitometric scanning of the [^{32}P] signals and normalization for AQP2 expression levels (Figure 5A, IB) revealed that with or without stimulation, the level of AQP2-R254L phosphorylation was only approximately 2% of that of unstimulated wt-AQP2 and that forskolin increased wt-AQP2 phosphorylation 2.5-fold (Figure 5B).

These results indicated that the lack of phosphorylation at S256 by PKA might be the molecular reason for the impaired translocation of AQP2-R254L to the plasma membrane. Previously, we showed that AQP2-S256D mimics constitutively phosphorylated AQP2, as this protein even localizes in the apical membrane of MDCK cells without forskolin treatment (18,20). For determining whether the lack of phosphorylation was the only reason for AQP2-R254L to be involved in NDI, the S256D mutation was introduced into AQP2-R254L and transiently expressed in MDCK cells. CLSM analysis consistently revealed that AQP2-R254L-S256D was localized in the basolateral and apical membrane, besides some remaining vesicular expression (Figure 6). This localization was not influenced by forskolin treatment (data not shown).

Discussion

Lack of S256 Phosphorylation Likely Is the Molecular Cause of Dominant NDI Caused by AQP2-R254L

Here, we identified a novel mutation in the AQP2 gene of a patient with dominant NDI. Our data indicate that, similar to other AQP2 mutants in dominant NDI (5–8,10), the encoded AQP2-R254L mutant protein causes dominant NDI by inhibiting the trafficking of wt-AQP2 to the apical membrane of the

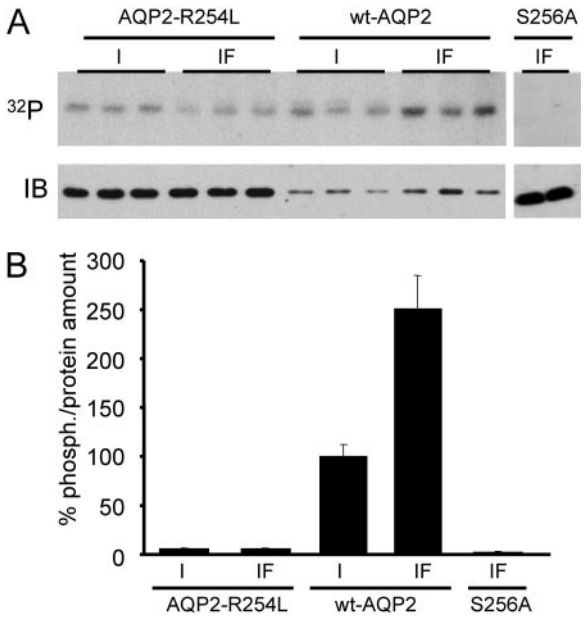

Figure 5. (A) Phosphorylation of AQP2-R254L in MDCK cells. Cells expressing wt-AQP2, AQP2-R254L, or AQP2-S256A were grown, and triplicates from each cell line were treated with indomethacin (I) or indomethacin/forskolin (IF), as described in the legend of Figure 3, and subjected to [^{32}P]orthophosphate labeling. After cell lysis, the AQP2 proteins were immunoprecipitated, split into two portions, one of which was separated on SDS-PAGE and autoradiographed (^{32}P), whereas the second was immunoblotted for AQP2 (IB). (B) Semiquantification of the level of AQP2-R254L phosphorylation. The [^{32}P] and immunoblot signals of AQP2 in A were densitometrically scanned and normalized against the AQP2 protein expression levels. Bars represent the ratio of phosphorylated AQP2 normalized for the total amount of that particular AQP2. The level of phosphorylation as found for wt-AQP2 incubated with indomethacin was set to 100%.

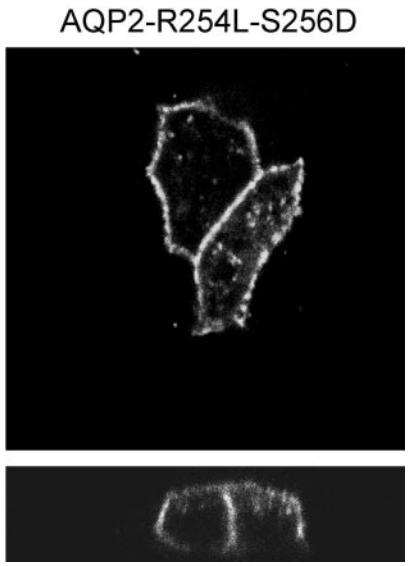

Figure 6. AQP2-R254L-S256D expression in MDCK cells. Polarized MDCK cells that transiently expressed AQP2-R254L-S256D were incubated in normal medium, fixed, immunostained for AQP2 proteins, and subjected to CLSM analysis as described in the legend of Figure 4A. Independent of forskolin treatment, AQP2-R254L-S256D was localized mainly in the apical and basolateral membrane, whereas some was retained in intracellular vesicles.

principal cells of the patient, because of the following: Upon expression in oocytes and MDCK cells, AQP2-R254L was a functional water channel but was retained in the cell. However, it was not retained in the ER, as a 32-kD high-mannose glycosylation band, which is characteristic for ER-retained AQP2 mutants in recessive NDI (13,24,25), was not observed (Figure 2). Also, AQP2-R254L formed heteroligomers with wt-AQP2 in oocytes (Figure 2) and MDCK cells (Figure 4C) and impaired the further trafficking of wt-AQP2 to the plasma membrane (Figure 4B).

Our data also indicate that the lack of phosphorylation of AQP2-R254L at S256 is the major, if not only, molecular cause of NDI in this family. At first, AQP2-R254L was retained to a similar extent and gave similar water permeability in oocytes as AQP2-S256A (Figure 2). In addition, AQP2-R254L, AQP2-S256A, and unstimulated wt-AQP2 (the majority of wt-AQP2 is unphosphorylated) seemed to localize to the same compartments in MDCK cells, as they all partially co-localized with EEA1, an endosomal marker protein (Figure 4A), whereas none of them localized to the ER, cis-median Golgi complex, trans-Golgi network, late endosomes/lysosomes, or basolateral membrane (data not shown). Most convincing, however, forskolin treatment did not increase phosphorylation of AQP2-R254L or AQP2-S256A, in contrast to wt-AQP2 (Figure 5, A and B), and introduction of "constitutive phosphorylation," as realized with AQP2-R254L-S256D, clearly shifted its expression from intracellular vesicles to the plasma membrane (Figure 6).

Although the osmolality of 452 obtained after saline infusion should be interpreted with caution because we did not measure the volume of saline infused, the concomitant increase in plasma sodium, or the Na+K content of the urine, infusion with hypertonic saline and hydrochlorothiazide seemed to improve the urine-concentrating ability of the proband. In lithium-NDI rats, hydrochlorothiazide seemed to improve the urine-concentrating ability, which coincided with increased AQP2 expression levels (26). If hydrochlorothiazide also increases AQP2 expression in humans, then this might indicate that NDI caused by retention of wt-AQP2 as a result of its interaction with AQP2-R254L might be partially overcome by an increased expression, as a higher level of AQP2-R254L expression resulted in a higher level of water permeability (Figure 2).

Using antibodies that recognize p-AQP2, it has been shown that AQP2 is phosphorylated at S256 *in vivo* (27,28) and that phosphorylation of AQP2 at S256 is essential for its trafficking to the plasma membrane *in vitro* (18–21). Because AQP2-R254L is impaired in its phosphorylation of S256 and causes dominant NDI, it reveals for the first time the fundamental importance of AQP2 phosphorylation at S256 *in vivo*.

The Kinase That Phosphorylates S256 in AQP2

Because S256 is part of a cAMP-dependent PKA phosphorylation consensus site [$(R/K)_2$-X-S/T] and AVP in collecting ducts is known to induce a cAMP signaling cascade, it is widely assumed that AQP2 is phosphorylated by PKA. However, the necessity for cytosolic calcium and activated calmodulin in AVP-induced AQP2 translocation to the plasma membrane of primary collecting duct cells (29) suggests that AQP2 might also be phosphorylated by the calcium-sensitive calmodulin kinase II (CaMKII), which is expressed in renal principal cells (30) and the consensus site (R-X-X-X-S/T-X [31]) of which also fits the Ser256 region. In addition, the Ser256 region conforms to the consensus site for cGMP-dependent protein kinase G [PKG; $(R/K)_{2-3}$-X-S/T-X (31)], and Bouley *et al.* (32) recently reported that nitric oxide and atrial natriuretic factor stimulate cGMP-dependent phosphorylation and plasma membrane insertion of AQP2 in kidney slices and cultured $LLCPK_1$-AQP2 cells.

Our study provides further evidence that PKA indeed mediates the AVP-mediated phosphorylation of AQP2. Because forskolin increases the levels of cAMP in MDCK-AQP2 cells (17) but not of calcium (data not shown) and the R254L mutation destroys the PKA consensus site but not those of CaMKII or PKG, the forskolin-induced phosphorylation of wt-AQP2 but not of AQP2-R254L indicates that wt-AQP2 phosphorylation by AVP is mediated *via* PKA. However, the basal level of phosphorylation of AQP2-R254L, in which the PKA consensus site thus is destroyed, indicates that other kinases also can phosphorylate AQP2. Although other putative sites in AQP2-R254L can not be excluded, the site phosphorylated in AQP2-R254L most likely is S256 for the following reasons. First, in the same orthophosphate labeling experiment (Figure 5), AQP2-S256A was not phosphorylated by forskolin, but its expression level was higher than that of wt-AQP2 or AQP2-R254L. Second, of all of the putative Ser/Thr phosphorylation sites in AQP2, only S256 seemed to have a role in AQP2 trafficking and forskolin-induced translocation of AQP2 to the plasma membrane (18–21). Third, treatment with the protein kinase C activator 4β-12-O-tetradecanoylphorbol-13-acetate in combination with forskolin induced the internalization of phosphorylated wt-AQP2 as well as AQP2-S256D. Using orthophosphate labeling assays and antibodies that recognize S256 phosphorylation, however, phosphorylation of a site other than S256 was never detected (18).

Although PKG (and other unknown kinases) cannot be excluded, the basal level of phosphorylation of AQP2-R254L might be mediated by CaMKII, as its consensus site is still intact in AQP2-R254L and the presence of calcium is also essential for AQP2 translocation in MDCK cells (F. Detmers and P.D., unpublished data). It remains to be determined, however, whether wt-AQP2 is phosphorylated at a basal level by other kinases and, if so, whether this has a physiologic role in the regulation of AQP2.

Basolateral Targeting of Phosphorylated AQP2-R254L

Epithelial cells have distinct apical and basolateral membranes with different protein compositions. This asymmetry is critical for their function and results from sorting mechanisms that recognize specific sorting signals. Basolateral signals include tyrosine motifs (NPXY or YXXØ), as well as dileucine and dihydrophobic residues (33,34). The R254L mutation, however, does not introduce a dileucine or dihydrophobic motif, as position 254 is flanked by an arginine and a glutamine. However, recent reports indicate that a single leucine can also mediate basolateral sorting, as the basolateral expression of the stem cell factor and CD147 also depend on the presence of a single leucine residue in their C-terminal tails (35,36). In addition, another AQP2 mutant in dominant NDI (AQP2-insA) was targeted to the basolateral membrane because of two newly introduced basolateral sorting signals in the AQP2 C-terminus. These signals included a monoleucine at L259, which by itself was sufficient for a complete basolateral expression of the AQP2 mutant (6). Because AQP2-S256D is expressed only in the apical membrane (18) and the apical sorting information of AQP2 is contained in the proximal region of its C tail (37), the even distribution of AQP2-R254L-S256D over the apical and basolateral membrane (Figure 6) indicates that the basolateral sorting signal formed by L254 in AQP2-R254L is weaker than L259 in AQP2-insA to overrule the apical sorting signal(s) in AQP2, which might contribute to the partial ability of the patient to concentrate urine with hypertonic saline and thiazide. Similarly, the retention of the AQP2-P262L mutant in intracellular vesicles was overcome by co-expression of and interaction with wt-AQP2, which explained the involvement of AQP2-P262L in recessive instead of dominant NDI (38). These data indicate that the severity of NDI in patients with dominant NDI depends to great extent on the strength by which an AQP2 mutant protein is able to prevent trafficking of wt-AQP2/mutant heteromeric complexes to the apical membrane and suggests that a single copy of some mutations in AQP2 may contribute to individual variation in ability to concentrate urine.

Acknowledgments

This research was supported by grants from the Dutch Organization of Scientific Research (NWO-MW 902-18-292 to P.M.T.D. and P.v.d.S. and NWO 916-36-122 to E.J.K.) and from the European Union (QLRT-2000-00778; QLK3-CT-2001-00987) and Kidney Foundation (PC159) to P.M.T.D.

We gratefully acknowledge Drs. S. Nielsen (Aarhus, Denmark), Y. Ikehara (Fukuoka, Japan), I. Braakman (Utrecht, The Netherlands), and Le Bivic (Marseille, France) for their kind gifts of antibodies against p-AQP2, GOS28 and Giantin, protein disulphide isomerase, and Lamp2, respectively. We are indebted to Dr. Erhard Klauschenz (Berlin, Germany) and Bärbel Mohs for DNA sequence analysis and Dr. Herbert J. Kramer (Bonn, Germany) for providing blood samples.

References

1. Deen PMT, Marr N, Kamsteeg EJ, Van Balkom BWM: Nephrogenic diabetes insipidus. *Curr Opin Nephrol Hypertens* 9: 591–595, 2000
2. Nielsen S, Chou CL, Marples D, Christensen EI, Kishore BK, Knepper MA: Vasopressin increases water permeability of kidney collecting duct by inducing translocation of

aquaporin-CD water channels to plasma membrane. *Proc Natl Acad Sci U S A* 92: 1013–1017, 1995
3. Deen PMT, Verdijk MAJ, Knoers NVAM, Wieringa B, Monnens LAH, van Os CH, van Oost BA: Requirement of human renal water channel aquaporin-2 for vasopressin-dependent concentration of urine. *Science* 264: 92–95, 1994
4. Mulders SM, Knoers NVAM, van Lieburg AF, Monnens LAH, Leumann E, Wuhl E, Schober E, Rijss JPL, van Os CH, Deen PMT: New mutations in the AQP2 gene in nephrogenic diabetes insipidus resulting in functional but misrouted water channels. *J Am Soc Nephrol* 8: 242–248, 1997
5. Mulders SM, Bichet DG, Rijss JPL, Kamsteeg EJ, Arthus MF, Lonergan M, Fujiwara M, Morgan K, Leijendekker R, van der Sluijs P, van Os CH, Deen PMT: An aquaporin-2 water channel mutant which causes autosomal dominant nephrogenic diabetes insipidus is retained in the Golgi complex. *J Clin Invest* 102: 57–66, 1998
6. Kamsteeg EJ, Bichet DG, Konings IB, Nivet H, Lonergan M, Arthus MF, van Os CH, Deen PMT: Reversed polarized delivery of an aquaporin-2 mutant causes dominant nephrogenic diabetes insipidus. *J Cell Biol* 163: 1099–1109, 2003
7. Kamsteeg EJ, Wormhoudt TA, Rijss JPL, van Os CH, Deen PMT: An impaired routing of wild-type aquaporin-2 after tetramerization with an aquaporin-2 mutant explains dominant nephrogenic diabetes insipidus. *EMBO J* 18: 2394–2400, 1999
8. Kuwahara M, Iwai K, Ooeda T, Igarashi T, Ogawa E, Katsushima Y, Shinbo I, Uchida S, Terada Y, Arthus MF, Lonergan M, Fujiwara TM, Bichet DG, Marumo F, Sasaki S: Three families with autosomal dominant nephrogenic diabetes insipidus caused by aquaporin-2 mutations in the C-terminus. *Am J Hum Genet* 69: 738–748, 2001
9. Asai T, Kuwahara M, Kurihara H, Sakai T, Terada Y, Marumo F, Sasaki S: Pathogenesis of nephrogenic diabetes insipidus by aquaporin-2 C-terminus mutations. *Kidney Int* 64: 2–10, 2003
10. Marr N, Bichet DG, Lonergan M, Arthus MF, Jeck N, Seyberth HW, Rosenthal W, van Os CH, Oksche A, Deen PMT: Heteroligomerization of an aquaporin-2 mutant with wild-type aquaporin- 2 and their misrouting to late endosomes/lysosomes explains dominant nephrogenic diabetes insipidus. *Hum Mol Genet* 11: 779–789, 2002
11. Oksche A, Dickson J, Schulein R, Seyberth HW, Muller M: Two novel mutations in the vasopressin V2 receptor gene in patients. *Biochem Biophys Res Commun* 205: 552–557, 1994
12. Bichet DG, Arthus M-F, Lonergan M, Hendy GN, Paradis AJ, Fujiwara TM, Morgan K, Gregory MC, Rosenthal W, Didwania A, *et al.*: X-linked nephrogenic diabetes insipidus mutations in North America and the Hopewell hypothesis. *J Clin Invest* 92: 1262–1268, 1993
13. Marr N, Bichet DG, Hoefs S, Savelkoul PJ, Konings IB, De Mattia F, Graat MP, Arthus MF, Lonergan M, Fujiwara TM, Knoers NVAM, Landau D, Balfe WJ, Oksche A, Rosenthal W, Muller D, van Os CH, Deen PMT: Cell-biologic and functional analyses of five new aquaporin-2 missense mutations that cause recessive nephrogenic diabetes insipidus. *J Am Soc Nephrol* 13: 2267–2277, 2002
14. Kamsteeg EJ, Deen PMT: Detection of aquaporin-2 in the plasma membranes of oocytes: A novel isolation method with improved yield and purity. *Biochem Biophys Res Commun* 282: 683–690, 2001
15. Deen PMT, Nielsen S, Bindels RJM, van Os CH: Apical and basolateral expression of aquaporin-1 in transfected MDCK and LLC-PK cells and functional evaluation of their transcellular osmotic water permeabilities. *Pflugers Arch* 433: 780–787, 1997
16. Deen PMT, Van Balkom BWM, Savelkoul PJ, Kamsteeg EJ, Van Raak M, Jennings ML, Muth TR, Rajendran V, Caplan MJ: Aquaporin-2: COOH terminus is necessary but not sufficient for routing to the apical membrane. *Am J Physiol Renal Physiol* 282: F330–F340, 2002
17. Deen PMT, Rijss JPL, Mulders SM, Errington RJ, van Baal J, van Os CH: Aquaporin-2 transfection of Madin-Darby canine kidney cells reconstitutes vasopressin-regulated transcellular osmotic water transport. *J Am Soc Nephrol* 8: 1493–1501, 1997
18. Van Balkom BWM, Savelkoul PJ, Markovich D, Hofman E, Nielsen S, van der Sluijs P, Deen PMT: The role of putative phosphorylation sites in the targeting and shuttling of the aquaporin-2 water channel. *J Biol Chem* 277: 41473–41479, 2002
19. Fushimi K, Sasaki S, Marumo F: Phosphorylation of serine 256 is required for cAMP-dependent regulatory exocytosis of the aquaporin-2 water channel. *J Biol Chem* 272: 14800–14804, 1997
20. Kamsteeg EJ, Heijnen I, van Os CH, Deen PMT: The subcellular localization of an aquaporin-2 tetramer depends on the stoichiometry of phosphorylated and nonphosphorylated monomers. *J Cell Biol* 151: 919–930, 2000
21. Katsura T, Gustafson CE, Ausiello DA, Brown D: Protein kinase A phosphorylation is involved in regulated exocytosis of aquaporin-2 in transfected LLC-PK1 cells. *Am J Physiol* 41: F816–F822, 1997
22. Kamsteeg EJ, Mulders SM, Bichet DG, Deen PMT, van Os C: Consequences of aquaporin 2 tetramerization for genetics and routing. *Nephrol Dial Transplant* 15[Suppl 6]: 26–28, 2000
23. Marr N, Kamsteeg EJ, Van Raak M, van Os CH, Deen PMT: Functionality of aquaporin-2 missense mutants in recessive nephrogenic diabetes insipidus. *Pflugers Arch* 442: 73–77, 2001
24. Deen PMT, Croes H, van Aubel RA, Ginsel LA, van Os CH: Water channels encoded by mutant aquaporin-2 genes in nephrogenic diabetes insipidus are impaired in their cellular routing. *J Clin Invest* 95: 2291–2296, 1995
25. Boccalandro C, De Mattia F, Guo DC, Xue L, Orlander P, King TM, Gupta P, Deen PMT, Lavis VR, Milewicz DM: Characterization of an aquaporin-2 water channel gene mutation causing partial nephrogenic diabetes insipidus in a Mexican family: Evidence of increased frequency of the mutation in the town of origin. *J Am Soc Nephrol* 15: 1223–1231, 2004
26. Kim GH, Lee JW, Oh YK, Chang HR, Joo KW, Na KY, Earm JH, Knepper MA, Han JS: Antidiuretic effect of hydrochlorothiazide in lithium-induced nephrogenic diabetes insipidus is associated with upregulation of aquaporin-2, Na-Cl co-transporter, and epithelial sodium channel. *J Am Soc Nephrol* 15: 2836–2843, 2004
27. Nishimoto G, Zelenina M, Li D, Yasui M, Aperia A, Nielsen S, Nairn AC: Arginine vasopressin stimulates phosphorylation of aquaporin-2 in rat renal tissue. *Am J Physiol* 276: F254–F259, 1999
28. Christensen BM, Zelenina M, Aperia A, Nielsen S: Local-

ization and regulation of PKA-phosphorylated AQP2 in response to V(2)-receptor agonist/antagonist treatment. *Am J Physiol Renal Physiol* 278: F29–F42, 2000
29. Chou CL, Yip KP, Michea L, Kador K, Ferraris JD, Wade JB, Knepper MA: Regulation of aquaporin-2 trafficking by vasopressin in renal collecting duct: Roles of ryanodine-sensitive Ca2+ stores and calmodulin. *J Biol Chem* 275: 36839–36846, 2000
30. Kubokawa M, Wang W, McNicholas CM, Giebisch G: Role of Ca2+/CaMK II in Ca(2+)-induced K+ channel inhibition in rat CCD principal cell. *Am J Physiol* 268: F211–F219, 1995
31. Blom N, Gammeltoft S, Brunak S: Sequence and structure-based prediction of eukaryotic protein phosphorylation sites. *J Mol Biol* 294: 1351–1362, 1999
32. Bouley R, Breton S, Sun T, McLaughlin M, Nsumu NN, Lin HY, Ausiello DA, Brown D: Nitric oxide and atrial natriuretic factor stimulate cGMP-dependent membrane insertion of aquaporin 2 in renal epithelial cells. *J Clin Invest* 106: 1115–1126, 2000
33. Bonafacino JS, Dell'Angelica EC: Molecular bases for the recognition of tyrosine-based sorting signals. *J Cell Biol* 145: 923–926, 1999
34. Rodionov DG, Nordeng TW, Kongsvik TL, Bakke O: The cytoplasmic tail of CD1d contains two overlapping basolateral sorting signals. *J Biol Chem* 275: 8279–8282, 2000
35. Wehrle-Haller B, Imhof BA: Stem cell factor presentation to c-Kit. Identification of a basolateral targeting domain. *J Biol Chem* 276: 12667–12674, 2001
36. Deora AA, Gravotta D, Kreitzer G, Hu J, Bok D, Rodriguez-Boulan E: The basolateral targeting signal of CD147 (EMMPRIN) consists of a single leucine and is not recognized by retinal pigment epithelium. *Mol Biol Cell* 15: 4148–4165, 2004
37. van Balkom BW, Graat MP, Van Raak M, Hofman E, van der SP, Deen PMT: Role of cytoplasmic termini in sorting and shuttling of the aquaporin-2 water channel. *Am J Physiol Cell Physiol* 286: C372–C379, 2004
38. De Mattia F, Savelkoul PJ, Bichet DG, Kamsteeg EJ, Konings IB, Marr N, Arthus MF, Lonergan M, van Os CH, van der SP, Robertson G, Deen PM: A novel mechanism in recessive nephrogenic diabetes insipidus: Wild-type aquaporin-2 rescues the apical membrane expression of intracellularly retained AQP2-P262L. *Hum Mol Genet* 13: 3045–3056, 2004

See related editorial, "Molecular Physiology of Renal Aquaporins and Sodium Transporters: Exciting Approaches to Understand Regulation of Renal Water Handling," on pages 2827–2829.